Spatio-temporal analysis of Highly Pathogenic Avian Influenza HPAI (H5N1) in poultry in Menofia governorate, Egypt

Yumna Elsobky (yumna.elsobky@vet.usc.edu.eg)
University of Sadat City
Mahmoud Eltholth
Royal Holloway University of London
Ehsan Abdalla
Tuskegee University
Nourhan Eissa
University of Sadat City
Ghada Hadad
University of Sadat City
Mohamed Nayel
University of Sadat City
Akram Salama
University of Sadat City
Walid Mousa
University of Sadat City
Ahmed Kamal
University of Sadat City
Mohamed Elkamshishi
Matrouh University

Research Article

Keywords: Highly pathogenic avian influenza (subtype H5N1), Epidemic waves, Spatio-temporal epidemiology, poultry population, Egypt

Posted Date: May 23rd, 2023

DOI: https://doi.org/10.21203/rs.3.rs-2948767/v1

Abstract

Background: Menofia governorate is one of Lower Egypt's governorates where the probability of zoonotic transmission of the H5N1 pandemic was high. This study aimed to investigate the spatiotemporal pattern, identify, and trace the highest risk clusters of HPAI H5N1 outbreaks at the subdistrict/village level in Menofia governorate, from 2006 to 2017 as a trial for tracking the HPAI H5N1 endemicity dynamics for better establishment of effective disease control strategies at that level.

Results: The epidemic curve in Menofia was similar to the national curve. Although the poultry population in Menofia was affected earlier than other places, the 1st Epidemic Wave (EW) started one week after the initial outbreak in Egypt, the HPAI H5N1 outbreaks never initiated from Menofia in all EWs. The outbreaks' spatial risk increases at the northern governorate border with a decrease in the spatial risk by the 6th EW. The hot spot region in Menofia was found in rural districts, especially villages, while outbreak density decreased with increased urbanization. Observed smoothed densities describe epidemic spread dynamics where the infection spreads and connects many different locations inside the same city, before jumping to new areas and directly connecting the nearest neighbor cities. The primary clusters could be predicted since they occur in the same areas where the highest relative risk clusters were recorded in the previous wave. Identifying continuous pinpointing clusters that persist for a long time, possibly spanning months, indicates the local transmission of the virus among poultry due to contact and widespread circulation. It is crucial to take early measures to prevent outbreaks at the initial sites before the outbreak acceleration phase, in order to minimize the geographic spread and confine the infection to specific areas. That suggests the need for the establishment of effective disease control strategies at the subdistrict level based on a better understanding of the endemicity dynamics.

Introduction

Highly pathogenic avian influenza (HPAI) subtype H5N1 is a potentially serious pandemic virus threatening the poultry industry in many developing countries because of its ability to evolve through genetic drifts [1]. In 2006, Egypt was the second African country to report HPAIH5N1 infection in poultry [2, 3]. Despite continuous governmental initiatives to limit the spread of the infection, HPAI H5N1 is endemic and has sever impacts on poultry industry and public health [4, 5]. Egypt has the highest number of HPAI H5N1 notifications of positive human cases between 2003 and 2017[6, 7] and the most important epicenter for HPAI H5N1 epidemic in Africa [8].

In Egypt, HPAI H5N1clade 2.2 was discovered for the first time in poultry in February 2006, since then, it has spread quickly across both backyard and commercial flocks [2, 3]. Since 2006, four major epidemic waves have been published in the poultry population [9]. Clade 2.2.1 was detected in all strains collected during the first wave between 2006 and 2007 [10], with the emergence of a new variant (clade 2.2.1.1), which was thought to be vaccine-driven [9]. HPAI H5N1 continued to spread among vaccinated backyard and commercial poultry initiating the second epidemic wave that lasted until 2008 and causing sever social and economic losses[11]. Egypt had been declared an Avian influenza endemic country in 2008

with the continuous evolution of the viruses [12]. Between 2008 to 2011, H5N1 variant clade 2.2.1.1 split into two different clusters (2.2.1.1 and 2.2.1.1a) [13]. The first cluster (2.2.1.1) was circulating from late 2007 till 2009, while the second cluster (2.2.1.1a) emerged in 2008 and persisted until 2011. Since then, no other instances of these variant clusters have been found [13]. However a new variant cluster was reported (subclade 2.2.1.2) in the early 2014, no significant alterations were found in the circulating viruses until 2016 [14, 15].

Egypt has a substantial poultry production sector where most poultry production is from Lower Egypt [9]. The majority of reported outbreaks in poultry were concentrated in the Nile Delta region, where high densities of poultry populations and activities were declared alongside an existing dense human population [9, 16–19]. Menoufia governorate has the highest number of poultry cases compared with other Egyptian governorates [19, 20]. It possesses the most productive land of the delta, where most of the population lives in villages and small towns. Agriculture is the principal occupation, employing more than 60% of the workers, and agricultural activities are supporting the dense rural population [21]. One of the agricultural activities is poultry breeding and live bird marketing, either small commercial poultry farms or backyard poultry. Backyard poultry in rural regions is a significant source of affordable protein and small businesses' financial resources [17].

Furthermore, the various well-structured poultry production sectors present in the Menofia governorate lack adequate production capabilities to meet the significant nutritional needs of the population. As a result, there has been a rise in unregistered and disorganized concentrated small-scale poultry producers, posing a significant risk for the occurrence and spread of poultry diseases. (Sheta et al., 2014). Unregulated production and of both commercial and household poultry, HPAI H5N1 infection is circulated without geographical barriers [9, 22, 23]. Although a higher rate of HPAI H5N1 outbreaks had been notified since 2006 in the Nile Delta region, it doesn’t fully reflect the true widespread endemic situation of the virus in the region due to the prevailing policy of under-reporting of the disease in the commercial sector in an attempt to protect their business interests and to prevent the mass culling of poultry stocks [20, 24].

The absence of detailed meaningful epidemiological investigations is a major obstacle, hindering the integrity of established control strategies [24]. This absence urges the appearance of certain studies concerned with both the temporal and spatial patterns of HPAI H5N1 outbreaks in different Egyptian governorates [7–9, 17, 22, 25–27]. Spatio-temporal analysis of HPAI H5N1 had been performed to reveal the geographic distribution, spatial and temporal dynamics of the HPAI outbreaks in India [28]. Due to the lack of granular data for outbreaks, scan statistics were used to enable the detection of clusters and guide disease control intervention [28].

Aggregated data at country/sub-district centroids may occasionally mask smaller clusters with high risk [19, 29]. As a result, the detection of the spatial cluster of outbreaks could have been made accurately when involving finer detailed data in sub-districts within villages, and more reliable surveillance data in addition to up-to-date reported outbreak data [28]. This study aimed to investigate the spatiotemporal pattern, identify, and trace the highest risk clusters of HPAI H5N1 outbreaks in Menofia governorate, from

2006 to 2017. This is a trial for tracking the HPAI H5N1 endemicity dynamics for better establishment of effective disease control strategies at subdistrict/village level.

Data and methods

Description of the Study Area

The Nile delta region is about 40,000 km^2 where more than half of Egypt's inhabitants live along with large numbers of poultry that are raised, traded, and consumed [30]. The scope of this study is Menoufia governorate, reported to have the highest disease incidences of HPAI [13]. Menoufia is one of the leading poultry-producing governorates in Egypt [31], where registered and unregistered commercial farms were found, in addition to the backyard which are random dispersed small-sized household flocks of mixed birds of different species and different ages with various vaccination protocols [32, 33].

Data collection

In Menofia, 659 confirmed events of HPAI-H5N1 outbreaks in domestic poultry were officially reported to the Global Animal Disease Information System (EMPRES-I) provided by FAO [FAO, 34], and the Egyptian ministry of agriculture (General Organization For Veterinary Services) official reports for national surveillance from January 2006 to December 2017.

All data were integrated into one dataset and the villages were used as an administrative unit.

The term outbreak was defined as *'the confirmed presence of disease with a clinical expression or not, in at least one individual in a defined location during a specified period'* [35]. The epidemic date and the outbreak centroids were utilized as spatiotemporal characteristics of each outbreak. The governorate map was constructed by (ArcGIS) to facilitate the presentation of data and the interpretation of results.

Method of analysis

Daily, weekly, and monthly epidemic curves, were constructed to display outbreak magnitude and temporal trends of HPAI-H5N1 outbreaks. An epidemic wave (EW) is a number of disease outbreaks that rapidly peaked and then gradually decreased till the end of the epidemic [36], and the number of outbreaks was calculated for each EW.

The interpolation tools were used to study the HPAIH5N1 outbreak risk. A raster risk map displays the interpolated surface, providing predictions for each location. The geostatistical analysis surface was derived using ordinary kriging by weighting the surrounding of the reported outbreak events to derive a prediction for the unreported locations. The general formula is formed as a weighted sum of the data values [37]:

$$\widehat{Z}\left(\mathrm{S}_0\right) = \sum_{i=1}^{n} \lambda_i \mathrm{Z}\left(\mathrm{S}_i\right)$$

where:

Z(*si*) = the reported outbreaks at the *i*th location

λ*i* = an unknown weight for the number of outbreak events at the *i*th location

s_0 = the prediction location

n = the number of outbreak events

Spatially kernel density analysis (KDE) is a simple non-parametric technique that relies on a few assumptions about the structure of the observed data [38]. It is equivalent to a simple diffusion model that is a useful approximation to patterns of distribution frequently found in ecological data [39]. KDE was used to identify high-density areas [40]; run in **Environmental Systems Research Institute** ArcMap 10.5 software using reported cases to generate a density surface for each EW.

The quartic kernel function [41, 42] is given by:

$$\hat{}_i(S) = \sum_{d_{i \le \tau}} \frac{3}{\pi \tau^2} \left(1 - \frac{d_i^2}{\tau^2}\right)^2$$

where:

1. i = *1,…,n* are the input points.
2. d_i is the distance between the point s and the observed event in location,
3. s_i and τ is the radius centered on s.

The formula to calculate the bandwidth is as follows [ESRI, 43]:

$$SearchRadius = 0.9 * \min\left(SD, \sqrt{\frac{1}{In(2)}} * D_m\right) * n^{-0.2}$$

where:

- SD is the standard distance
- D_m is the median distance
- n is the number of points if no population field is used, or if a population field is supplied, n is the sum of the population field values

Kernel density maps for the total number of cases were plotted for each EW to visualize the risk for the disease. Default cells and the output were selected in Square kilometers (Km^2).

Retrospective space-time permutation scan statistics were performed to detect the Spatio-temporal clusters for each EW by investigating whether the outbreaks were interrelated in space and time using (SaTScan 8.2.1 software) [44–46]. The scanning window was a cylinder with the spatial and temporal dimensions as circular base and height, respectively. The temporal scanning window was set to < 50% of the study period in each EW and a maximum of 50% of outbreaks were allowed in the spatial scanning window [47].

The likelihood ratio statistic was used to evaluate the possibility of a true spatiotemporal cluster in a window. The window with the maximum likelihood ratio statistic was considered the primary cluster while the remainder were considered secondary clusters. Their statistical significance was tested through Monte Carlo simulations of 999 replications [47]. The time units of day, week, and month were used, respectively.

ArcGIS 10.5 software was used to overlay results from different methods in a map for visual comparisons **(ESRI, Redlands).**

Results

Temporal distribution of HPAI H5N1 outbreaks in Menofia governorate, Egypt

Six epidemic waves (EW1-6) of H5N1 outbreaks were noted throughout the study's period (2006–2017) Fig. 1. The 1st EW, in which the governorate reported 66 outbreaks, lasted for about three months, Fig. 1, started in February 2006, peaked in mid-March 2006, and ended in May 2006. In Fig. 1. the 2nd EW began on the 21st of November 2006, peaked in last December 2006, and ended in mid-April 2007, with 57 estimated outbreaks that lasted for four months. The third epidemic wave (3rd EW), Menofia governorate reported 30 outbreaks that lasted for three months, Fig. 1, began on December 2nd, 2007, peaked in the period from 22 December 2007 to 20 January 2008, and ended in mid-March 2008. The fourth epidemic wave (4th EW) considered one of the longest epidemic waves that reflects the endemic situation, started on December 16th, 2008, and ended on February 11th, 2012. Multiple consecutive peaks of the HPAI H5N1 outbreaks were continuously reported for more than three years with 378 reported outbreaks, Fig. 1. Four epidemic cycles were found, the first of which lasted from January 2009 to August 2009, the second of which lasted from January 2010 to August 2010, the third of which lasted from January 2011 to August 2011, and the last one peaked in January 2012. The fifth epidemic wave (5th EW) started in September 2012 and ended in late May 2013 with multiple consecutive peaks reported in October 2012, late November 2012, early February 2013, and mid-April 2013, with 58 reported outbreaks. While the sixth epidemic wave (6th EW) started in October 2013 and recorded 70 outbreaks continuously to December 10th, 2016. There was only one definitive peak observed in February 2015, Fig. 1.

Figure 2., and Fig. 3 declare the distribution of the numbers of outbreaks for each one of the six epidemic waves by localities. During the whole period of the study (Fig. 2A), the highest numbers of outbreaks have

been reported in Ashmun, Minuf, and Qwesna respectively. The second-highest category is Berkat_ElSabae, ElBagur and Shibin_ElKom followed by the third-highest category of Tala, ElShohadaa, and Sadat_City (Fig. 2A). According to Table 1, and Fig. 2B, most outbreaks in the 1st EW have been reported in Qwesna, Berkat ElSabae, and Ashmun with 34.8%, 18.2%, and 16.7% of total cases, respectively. As seen in Table 1, and Fig. 2C the largest number of outbreaks have been reported in the 2nd EW, were found in Berkat ElSabae, Minuf, and Shibin_ElKom with 28.1%, 15.8%, and 12.3% of total cases, respectively. The areas with the most outbreak notifications in 3rd EW are Ashmun, Shibin_ElKom, and Tala, with 33.3%, 26.7%, and 13.3% of total cases, respectively (Table 1 and Fig. 2D). The highest numbers of outbreaks in the governorate have been notified in 4th EW in Minuf, Ashmun, and Qwesna with 24.6%, 17.7%, and 14% of total cases, respectively (Table 1 and Fig. 2E). Ashmun has been reported to have the most outbreaks in the Menofia governorate in 5th EW with 43.1% of total cases, followed by Qwesna with 34.5% of total cases (Table 1 and Fig. 2F). The Menofia governorate has received the most outbreak notifications in Ashmun, Minuf, and Shibin_ElKom, correspondingly in 6th EW with 34.3%, 22.9%, and 12.9% of total cases, respectively (Table 1 and Fig. 2G).

The spatial pattern of HPAI H5N1 outbreak in Menofia governorate, Egypt

Spatial distribution of HPAI H5N1 outbreaks in Menofia governorate illustrated in Fig. 3, divided into six EW (epidemic waves) and depicted in the village-based map for visual comparison using ARCGIS 10.5 software (ESRI, Redlands, CA, USA).

Based on the raster risk map in Fig. 4, which displays the interpolated surface based on ordinary kriging, provides predictions of outbreak occurrence risk for each location in the Menofia governorate at each EW. Berkat ElSabae and Qwesna in the northeast border of the governorate were determined to have the highest predicted risk of HPAI H5N1 spatial occurrence in the 1st EW. In the next occurred wave, the outbreaks spread all over the governorate with a generally high density, the highest predicted risk was observed in the northeast part of the governorate (Berkat ElSabae and Qwesna cities) and extended risk to the center of the governorate (Minuf, ElShohadaa, and Shibin_ElKom cities) to Ashmun city. While at the 3rd EW, the northeast part of the governorate (Berkat ElSabae and Qwesna cities) had the lowest predicted risk of HPAI H5N1 occurrence. The spatial highest predicted risk was noted in the northwestern borders of the governorate (Tala city), extended to the center (Shibin_ElKom city), and down to Ashmun city. In the 4th EW, the outbreaks spread with the highest predicted risk at the north governorate borders. While in the 5th EW, the outbreaks spread all over the governorate with the highest predicted risk at the north and south governorate borders. However, in the 6th EW, a generally low density was detected with the highest predicted risk at Minuf, and ElBagur.

In the current study, outbreak density and cluster analysis of HPAI H5N1 outbreaks over six epidemic waves in Menofia governorate were depicted in Table (2, 3) and Fig. (5). Outbreak density in the Menofia governorate was determined by adaptive kernel density estimation, highlighted in monochromatic grey (the higher the density, the darker the color) and outbreaks were represented by green dots. The first

epidemic wave (1st EW) of outbreaks in the Menofia governorate had the highest outbreak density in Qwesna and Shibin_ElKom, while the second epidemic wave (2nd EW) had outbreak densities in Qwesna, Berkat ElSabae, ElShohadaa, Minuf, and Ashmun. The spread of the outbreak density during the third epidemic wave (3rd EW) covered Tala, Berkat ElSabae, Shibin_ElKom, and Ashmun. In the fourth epidemic wave (4th EW), the outbreaks covered the whole governorate with the highest densities found at Qwesna, Berkat ElSabae, ElBagur, and Ashmun. While in the fifth epidemic wave (5th EW), the spatial distribution of outbreaks was confined to Qwesna and Ashmun. By the sixth epidemic wave (6th EW), Qwesna, Shibin_ElKom, ElShohadaa, Minuf, and Ashmun had shown a high outbreak density.

Spatiotemporal clusters

Clustering is an aggregation of diseases in space and/or time in amounts that are believed to be greater than could be expected [48]. To determine the outbreak clusters at each EW, spatiotemporal cluster analysis is performed. The current study couldn't take into account various control measures, detection bias, or even changes in the demographic features of at-risk groups, and that is considered one of its limitations. Tables (2,3) and figure (5) provide a detailed description of the location and the extent of different clusters in the Menofia governorate.

Throughout the six epidemic waves in the Menofia governorate, there were spatial patterns and spatiotemporal clusters of HPAI subtype H5N1 outbreaks that occurred on a daily, weekly, and monthly basis. Significant spatiotemporal clusters detected from the space-time permutation scan statistics are represented by the most likely cluster (red circle) and by a secondary cluster (blue dashed circles) in tables (2, 3) and figure (5).

Based on the daily and weekly outbreak data, the primary cluster, and the most likely occurring one in the 1st EW, was found in Tala city at the end of the wave. The secondary cluster in Tala city was also detected as the highest relative risk cluster, in addition to the one found in Tala, ElShohadaa, Shibin_ElKom, Minuf, Qwesna, and Berkat ElSabae at a 26.37 Km radius, based on monthly outbreak data. During the 2nd EW, the primary cluster of radius 6.56 km was observed in Tala, ElShohadaa, and Shibin_ElKom at the end of the wave, based on weekly and monthly outbreak data. While the primary cluster based on the daily outbreak data was observed in the same cities but with a bigger radius of 12.60 Km including Minuf city. The secondary clusters covered the whole governorate during 2nd EW, and the highest RR clusters were observed in small villages in Ashmun, ElBagur, and Shibin_ElKom.

In 3rd EW, the daily based outbreaks showed a primary cluster at the end of the wave of a 6.87 Km radius in ElBagur and Ashmun, while with the monthly outbreaks, the primary cluster and the most likely occurred one was found in Ashmun of a smaller radius (2.14 Km radius). Although the primary cluster with weekly outbreaks was detected in ElBagur, Shibin_ElKom, Qwesna, and Berkat ElSabae with a 9.29 Km radius at the end of the wave. The secondary clusters predominate the majority of the cities, and the most likely occurred clusters were found in the villages of Shibin_ElKom, Ashmun, Berkat ElSabae, and Tala. The primary cluster in 4th EW was located in ElBagur, Qwesna, and Shibin_ElKom at the middle of the wave, characterized by a 10.21 Km radius size as shown in Fig. 5, based on daily and weekly outbreak

data. While the analysis of monthly-based outbreaks showed a primary cluster of a smaller radius size of 5.17 Km in Qwesna and Berkat ElSabae. The secondary clusters occurred consecutively -one following the other- to cover the whole governorate geographic surface during the whole period of 4th EW. The secondary clusters of the highest relative risk were found mainly in Minuf and Tala.

At the end of the 5th EW, the primary cluster of a 14.01 Km radius was observed in Minuf, Ashmun, and ElBagur based on weekly outbreak data. The monthly based outbreaks showed smaller primary clusters of 6.46 Km in the same cities with the highest relative risk. While the primary cluster based on the daily outbreak data includes only Shibin_ElKom and Qwesna within a 4.04 Km radius. The highest relative risk (RR) secondary clusters were determined in Tala, Berkat ElSabae, Ashmun, and Minuf.

In the 6th EW, the primary clusters were observed to occur anytime during the wave with analysis of daily, weekly, and monthly outbreak data with secondary clusters that cover the whole governorate. The daily-based outbreaks showed primary clusters of a 7.97 Km radius in Minuf, and Ashmun at the end of 2014. While the monthly-based outbreaks showed a primary cluster of a 10.06 Km radius in Minuf, Shibin_ElKom, and ElBagur from January 2015 and lasted six months. The primary cluster according to the weekly based outbreak was detected in Tala, Berkat ElSabae, and Shibin_ElKom of a 6.02 Km radius at the end of 2015. Secondary clusters of high relative risk (RR) were determined in Ashmun, Qwesna, ElShohadaa, Shibin_ElKom, ElBagur, and Minuf which are almost all cities of the Menofia governorate.

Discussion

Our study aimed to investigate the spatiotemporal pattern, identify, and trace the highest risk clusters of HPAI H5N1 outbreaks at the subdistrict/village level within the Menofia governorate, from 2006 to 2017 as a trial for tracking the HPAI H5N1 endemicity dynamics for better establishment of effective disease control strategies at that level.

Epidemic waves of HPAI H5N1 outbreaks in Menofia governorate

Six epidemic waves (EWs) were represented by different time scales of day, week, and month and showed similar patterns indicating the strong epidemic feature of HPAI subtype H5N1. The duration of the EWs (1 to 6) was 3, 5, 3, 38, 7, and 39 months, respectively as illustrated in Fig. 1. The epidemic curve in Menofia follows the same patterns of six Egyptian epidemic waves according to previously published studies by [19, 49], and a global study by [50]. There is a noninterpreted epidemic cycle of the disease with the peak of the outbreaks at each EW usually found in December and January. The epidemic curve is characterized by a short vertical span and a long horizontal span confirming the endemic situation and suggesting an increase in outbreaks' spatial distribution over time in the governorate. According to the epidemic waves of HPAI H5N1 outbreaks in Egypt described by Y Elsobky, G El Afandi, A Salama, A Byomi, M Omar and M Eltholth [19], the poultry population in Menofia was the first to be affected since the 1st EW in Menofia governorate started one week after the disease's initial introduction in Egypt and

ended two months before the end of Egypt's first recorded epidemic wave. The 2.2.1 clade is the first described clade in the 1st EW, and it remained during the 2nd EW and 3rd EW. Besides the 2.2.1.1 clade that started in the 2nd EW was also represented during the 3rd EW then the disease became endemic in 2008 [51]. The 2nd EW, 3rd EW, 4th EW, and 5th EW in the Menofia governorate started one month after the start of the Egyptian epidemic waves. Although the 2nd EW, 3rd EW, 4th EW, and 5th EW in the Menofia governorate ended almost three months before the end of the Egyptian epidemic waves. Although the HPAI H5N1 outbreaks never being initiated from Menofia in all epidemic waves, it was considered one of the highest governorates to record outbreaks during those periods according to Y Elsobky, G El Afandi, A Salama, A Byomi, M Omar and M Eltholth [19]. This is probably because of the highest density of poultry population in the governorate. Our analysis indicates that the best control strategies should be directed to prevent the outbreak at the sites where the initiation phase starts before the outbreak acceleration phase.

Menofia governorate reported the highest outbreaks number during the 4th EW in Egypt with two recorded clades, clades 2.2.1.1a and 2.2.1.2 in association with the notification of H9N2 for the first time in 2009 [19, 51]. After that time, the 2.2.1.2 clade continues to circulate and show progressive adaptation to the poultry population [51]. It was also observed that during the 4th EW, outbreaks were first recorded in warmer months. In 4th EW, epidemic cycles are characterized by a wider horizontal span that reflects the longer circulation of the infection in the area. It is observed that the peaks of those epidemic cycles were earlier compared to the peaks of the fourth epidemic wave of Egypt, empathizing emerging of new clades from Menofia governorate. This would refer to the thermostability of newly emerged clades that can survive at warm temperatures [52]. It emphasizes the viral ability to maintain endemicity through adaptation [53]. Continuous notification of the outbreaks for more than half a year in 5th EW with the peaks without any clear patterns and with changes to the usual epidemic cycles, a way that confirms the viral adaptation and endemicity with the clades 2.2.1, 2.2.1.1a, and 2.2.1.2 were represented during the last two epidemic waves, this finding in agree with R El-Shesheny, A Kandeil, A Mostafa, MA Ali and RJ Webby [51]. The epidemic curve ended up with the 6th EW, without showing any definitive peak or any clear patterns at this period which is not reflecting the field situation of HPAI H5N1 outbreaks at that time. It probably could be due to the under-notification and weakness of the surveillance system to identify outbreaks. The same results of the 6th EW in Egypt by Y Elsobky, G El Afandi, A Salama, A Byomi, M Omar and M Eltholth [19].

The spatial pattern of outbreak density in Menofia governorate:

According to the majority of published studies on the geographic distribution of HPAI H5N1 in Egypt, the majority of poultry outbreaks are primarily concentrated in the densely populated Nile Delta region, with lower densities in upper Egypt [7, 11, 19, 54] where located dense concentration of poultry stocks and human population [16]. More than half of the Egyptian population is in close contact with raised poultry in the Nile Delta region [27]. As a result, Menofia governorate was one of Lower Egypt's governorates

identified as a significant substitute that would raise the probability of zoonotic transmission of the H5N1 pandemic, according to [7] study.

In Fig. 4, the HPAI H5N1 outbreaks' spatial risk increases at the governorate borders with the other provinces, especially the northern governorate border. Also, the risk increases in the areas that contain many small unlicensed farms and backyard poultry. These areas are believed to be randomly distributed in most of the Menofia cities. By the 6th EW, the spatial risk generally decreased because of the under-notification of the outbreaks. This requires the need for improving active surveillance and developing adequate synchronization between Egyptian governorates, so each one of them should be informed when an outbreak occurs in neighboring areas. A quick response plan to prevent disease spreading should include protecting borders, quarantining the villages where the outbreak occurs, hygienic disposal of dead birds, preventing the transportation of live birds, and live bird markets. Besides, maintaining proper vaccination coverage with proper biosecurity measures. Since HPAI H5N1 virus can survive and remain infectious at low temperatures for long periods in water or bird feces, for up to 102 days at 28˚C or up to 207 days at 17˚C in contaminated water [55], for 7 days at 20˚C and 30–35 days at 4˚C in liquid bird feces [56].

From kernel densities in Fig. 5, the hot spot region in Menofia is found in rural districts especially villages inside the delta region, it appears with the highest outbreak density in all the six epidemic waves. This is because of the relatively high number of household poultry, unorganized markets, registered and unregistered small poultry farms. While outbreaks density decreased with increased urbanization, that explains the lower densities found in localities with expanded urbanization such as main city zones and industrial zones such as Sadat City (a newly established urban community and one of the largest industrial cities in the country) as described by Gafı [57]. The observed smoothed densities describe the epidemic spread dynamics where the infection spreads and connects many different locations inside the same city, before jumping to new areas and directly connecting the nearest neighbor cities, the same as illustrated by [58]. This perspective indicates that the control measure is not effective in localizing the infection and controlling the outbreak spread. This refers to the importance of early actions to control the spread of disease successfully.

All the primary clusters in the first five EW as illustrated in Fig. 5, tables 2, and 3 are detected in the middle or at the end of the wave and mostly are the same areas of the highest relative risk clusters that occurred with the previous wave. They were also found in the hot-spot region while the location and the size of the cluster varied with each EW. The way it could be predicted to be controlled at the beginning of the wave is by more intense and strict actions in those areas to compress the spatial spread of the disease. In the last three EW, the secondary clusters appeared to occur consecutively to cover the whole governorate geographic surface. At the last EW, the primary clusters were observed to occur anytime during the wave with secondary clusters of high relative risk (RR) that cover the whole governorate. It is concluded from cluster analysis that outbreak clusters can be expected everywhere and anytime in the governorate and can last for an extended period that could be months. The distance between different clusters is short (2 km) with a time interval of (1 week) confirming the consecutive nature of the clusters, along with many

pinpointing clusters indicating the local spread through contact and the extensive circulation of the virus in the poultry population without successful interventions.

The applied control measures may have a short-term effect in lessening the disease spread and are ineffective in the spatial compressing of the disease or even controlling its epidemic strategy [1, 59]. This constitutes the need for the establishment of effective disease control strategies at the subdistrict level within each governorate based on a better understanding of the endemicity dynamics. Besides, the Egyptian veterinary authorities should evaluate their control strategies continuously and test them frequently with real field data [49]. While it is exceedingly challenging to get confirmed data of HPAI H5N1 outbreaks that represent the real field situation to be utilized in such epidemiological studies due to lack of notification, indirect effects of vaccination strategies, and/or compensation measures [19, 30, 49, 60, 61].

Declarations

Acknowledgments: Not applicable.

Consent for publication: Not applicable.

Competing interests: The authors declare that they have no competing interests.

Funding: This research did not receive any specific grant from funding agencies in the public, commercial, or not-for-profit sectors.

Ethical approval: The authors confirm that the ethical policies of the journal, as noted on the journal's author guidelines page, have been adhered to. No ethical approval was required as this is a research article with no original research data.

Availability of data and materials: All data generated or analyzed during this study are included in thispublished article.

Authors' contributions: Y. Elsobky the first author is the one who did the research and wrote the manuscript's first draft data collection and processing, and was a major contributor in cleaning, analysis, and interpretation. M. Eltholth and E. Abdalla have given significant intellectual inputs in the final revision and participated in the conceiving and designing of the manuscript. M. Nayel, A. Salama, and W. Mousa Made significant contributions to the cleaning and interpretation of the data. N. Eissa, G. Hadad, and A. Kamal participated in cleaning, and writing the manuscript. M. Elkamshishi participated in data collection, processing, and writing. All authors critically reviewed the manuscript and approved the final manuscript.

References

1. Otte J, Hinrichs J, Rushton J, Roland-Holst D, Zilberman D: **Impacts of avian influenza virus on animal production in developing countries**. *CAB Reviews: Perspectives in Agriculture, Veterinary Science, Nutrition and Natural Resources* 2008, **3**(080):18.
2. Aly M, Arafa A, Hassan M: **Epidemiological findings of outbreaks of disease caused by highly pathogenic H5N1 avian influenza virus in poultry in Egypt during 2006**. *Avian diseases* 2008, **52**(2):269-277.
3. Saad MD, Lu'ay SA, Gamal-Eldein MA, Fouda MK, Khalil FM, Yingst SL, Parker MA, Montevillel MR: **Possible avian influenza (H5N1) from migratory bird, Egypt**. *Emerging infectious diseases* 2007, **13**(7):1120.
4. Kalthoff D, Globig A, Beer M: **(Highly pathogenic) avian influenza as a zoonotic agent**. *Veterinary microbiology* 2010, **140**(3-4):237-245.
5. Matrosovich M, Zhou N, Kawaoka Y, Webster R: **The surface glycoproteins of H5 influenza viruses isolated from humans, chickens, and wild aquatic birds have distinguishable properties**. *Journal of virology* 1999, **73**(2):1146-1155.
6. Harfoot R, Webby RJ: **H5 influenza, a global update**. *Journal of microbiology* 2017, **55**(3):196-203.
7. Young SG, Kitchen A, Kayali G, Carrel M: **Unlocking pandemic potential: prevalence and spatial patterns of key substitutions in avian influenza H5N1 in Egyptian isolates**. *BMC infectious diseases* 2018, **18**(1):1-13.
8. Ekong P, Fountain-Jones N, Alkhamis M: **Spatiotemporal evolutionary epidemiology of H5N1 highly pathogenic avian influenza in West Africa and Nigeria, 2006–2015**. *Transboundary and emerging diseases* 2018, **65**(1):e70-e82.
9. Arafa A, El-Masry I, Khoulosy S, Hassan MK, Soliman M, Fasanmi OG, Fasina FO, Dauphin G, Lubroth J, Jobre YM: **Predominance and geo-mapping of avian influenza H5N1 in poultry sectors in Egypt**. *Geospatial health* 2016.
10. Balish AL, Davis CT, Saad MD, El-Sayed N, Esmat H, Tjaden JA, Earhart KC, Ahmed LaE, El-Halem MA, Ali AHM: **Antigenic and genetic diversity of highly pathogenic avian influenza A (H5N1) viruses isolated in Egypt**. *Avian diseases* 2010, **54**(s1):329-334.
11. Kayali G, Kandeil A, El-Shesheny R, Kayed AS, Maatouq AM, Cai Z, McKenzie PP, Webby RJ, El Refaey S, Kandeel A: **Avian influenza A (H5N1) virus in Egypt**. *Emerging infectious diseases* 2016, **22**(3):379.
12. El-Shesheny R, Kandeil A, Bagato O, Maatouq AM, Moatasim Y, Rubrum A, Song M-S, Webby RJ, Ali MA, Kayali G: **Molecular characterization of avian influenza H5N1 virus in Egypt and the emergence of a novel endemic subclade**. *The Journal of general virology* 2014, **95**(Pt 7):1444.
13. Arafa A, El-Masry I, Kholosy S, Hassan MK, Dauphin G, Lubroth J, Makonnen YJ: **Phylodynamics of avian influenza clade 2.2. 1 H5N1 viruses in Egypt**. *Virology journal* 2016, **13**(1):49.
14. Arafa A, Naguib M, Luttermann C, Selim A, Kilany W, Hagag N, Samy A, Abdelhalim A, Hassan M, Abdelwhab E: **Emergence of a novel cluster of influenza A (H5N1) virus clade 2.2. 1.2 with putative human health impact in Egypt, 2014/15**. *Eurosurveillance* 2015, **20**(13):21085.

15. Abdelwhab E, Hassan M, Abdel-Moneim A, Naguib M, Mostafa A, Hussein I, Arafa A, Erfan A, Kilany W, Agour M: **Introduction and enzootic of A/H5N1 in Egypt: Virus evolution, pathogenicity and vaccine efficacy ten years on**. *Infection, Genetics and Evolution* 2016, **40**:80-90.
16. Arafa A, Suarez D, Kholosy S, Hassan M, Nasef S, Selim A, Dauphin G, Kim M, Yilma J, Swayne D: **Evolution of highly pathogenic avian influenza H5N1 viruses in Egypt indicating progressive adaptation**. *Archives of virology* 2012, **157**(10):1931-1947.
17. El-Zoghby EF, Aly MM, Nasef SA, Hassan MK, Arafa A-S, Selim AA, Kholousy SG, Kilany WH, Safwat M, Abdelwhab E: **Surveillance on A/H5N1 virus in domestic poultry and wild birds in Egypt**. *Virology journal* 2013, **10**(1):1-10.
18. Sheta BM, Fuller TL, Larison B, Njabo KY, Ahmed AS, Harrigan R, Chasar A, Aziz SA, Khidr A-AA, Elbokl MM: **Putative human and avian risk factors for avian influenza virus infections in backyard poultry in Egypt**. *Veterinary microbiology* 2014, **168**(1):208-213.
19. Elsobky Y, El Afandi G, Salama A, Byomi A, Omar M, Eltholth M: **Spatiotemporal analysis of highly pathogenic avian influenza (H5N1) outbreaks in poultry in Egypt (2006 to 2017)**. *BMC Vet Res* 2022, **18**(1):174. DOI: 10.1186/s12917-022-03273-w.
20. Kayali G, Webby RJ, Ducatez MF, El Shesheny RA, Kandeil AM, Govorkova EA, Mostafa A, Ali MA: **The epidemiological and molecular aspects of influenza H5N1 viruses at the human-animal interface in Egypt**. *PloS one* 2011, **6**(3):e17730.
21. Britannica: **"Al-Minūfiyyah GOVERNORATE, EGYPT". britannica.** 2022. DOI: https://www.britannica.com/place/Al-Minufiyyah.
22. Abdelwhab E, Abdel-Moneim AS: **Epidemiology, ecology and gene pool of influenza A virus in Egypt: will Egypt be the epicentre of the next influenza pandemic?** *Virulence* 2015, **6**(1):6-18.
23. Abdelwhab E, Selim A, Arafa A, Galal S, Kilany W, Hassan M, Aly M, Hafez M: **Circulation of avian influenza H5N1 in live bird markets in Egypt**. *Avian diseases* 2010, **54**(2):911-914.
24. Farnsworth ML, Hamilton-West C, Fitchett S, Newman SH, de La Rocque S, De Simone L, Lubroth J, Pinto J: **Comparing national and global data collection systems for reporting, outbreaks of H5N1 HPAI**. *Preventive veterinary medicine* 2010, **95**(3-4):175-185.
25. Cattoli G, Fusaro A, Monne I, Coven F, Joannis T, Abd El-Hamid HS, Hussein AA, Cornelius C, Amarin NM, Mancin M: **Evidence for differing evolutionary dynamics of A/H5N1 viruses among countries applying or not applying avian influenza vaccination in poultry**. *Vaccine* 2011, **29**(50):9368-9375.
26. Hafez M, Arafa A, Abdelwhab E, Selim A, Khoulosy S, Hassan M, Aly M: **Avian influenza H5N1 virus infections in vaccinated commercial and backyard poultry in Egypt**. *Poultry science* 2010, **89**(8):1609-1613.
27. Abdelwhab E, Hafez H: **An overview of the epidemic of highly pathogenic H5N1 avian influenza virus in Egypt: epidemiology and control challenges**. *Epidemiology & Infection* 2011, **139**(5):647-657.
28. Dhingra MS, Dissanayake R, Negi AB, Oberoi M, Castellan D, Thrusfield M, Linard C, Gilbert M: **Spatio-temporal epidemiology of highly pathogenic avian influenza (subtype H5N1) in poultry in eastern India**. *Spatial and spatio-temporal epidemiology* 2014, **11**:45-57. DOI: 10.1016/j.sste.2014.06.003.

29. Jones SG, Kulldorff M: **Influence of spatial resolution on space-time disease cluster detection**. *PLoS One* 2012, **7**(10):e48036. DOI: 10.1371/journal.pone.0048036.
30. Abdelwhab EM, Hafez HM: **An overview of the epidemic of highly pathogenic H5N1 avian influenza virus in Egypt: epidemiology and control challenges**. *Epidemiology and infection* 2011, **139**(5):647-657. DOI: 10.1017/s0950268810003122.
31. ElMasry I, Elshiekh H, Abdlenabi A, Saad A, Arafa A, Fasina FO, Lubroth J, Jobre Y: **Avian influenza H5N1 surveillance and its dynamics in poultry in live bird markets, Egypt**. *Transboundary and emerging diseases* 2017, **64**(3):805-814.
32. Fasina FO, Ali A, Yilma J, Thieme O, Ankers P: **Production parameters and profitability of the Egyptian household poultry sector: a survey**. *World's Poultry Science Journal* 2016, **72**(1):178-188.
33. Ali A, Ankers P, DeHaan N, Saad A, Hussein S, Lubroth J, Jobre Y: **Mapping influenza A (H5N1) virus transmission pathways and critical control points in Egypt**. *FAO Animal Production and Health Working Paper* 2013(11).
34. Food and Agriculture Organization: **EMPRES-i-Global Animal Disease Information System. http://empres-i.fao.org/eipws3g/#h=0**. 2017.
35. Toma B, Benet J-JC, Duford BC, Eloit MC, Marsh WC, Michel PC, Moutou FC, Sanaa MC, Vaillancourt J-P: **Dictionary of veterinary epidemiology**. In.: Iowa State University Press; 1999.
36. Zhang Z, Chen D, Chen Y, Liu W, Wang L, Zhao F, Yao B: **Spatio-temporal data comparisons for global highly pathogenic avian influenza (HPAI) H5N1 outbreaks**. *PLoS One* 2010, **5**(12):e15314.
37. Oliver MA, Webster R: **Kriging: a method of interpolation for geographical information systems**. *International Journal of Geographical Information Systems* 1990, **4**(3):313-332. DOI: 10.1080/02693799008941549.
38. Worton BJ: **Kernel methods for estimating the utilization distribution in home-range studies**. *Ecology* 1989, **70**(1):164-168. DOI: https://doi.org/10.2307/1938423.
39. O'Brien SH, Webb A, Brewer MJ, Reid JB: **Use of kernel density estimation and maximum curvature to set Marine Protected Area boundaries: Identifying a Special Protection Area for wintering red-throated divers in the UK**. *Biological Conservation* 2012, **156**:15-21. DOI: https://doi.org/10.1016/j.biocon.2011.12.033.
40. Silverman BW: **Density estimation for statistics and data analysis (1st ed.)**: Routledge; 1998. DOI: https://doi.org/10.1201/9781315140919.
41. Bailey TC, Gatrell AC: **Interactive spatial data analysis**, vol. 413: Longman Scientific & Technical Essex; 1995. DOI: http://www.personal.psu.edu/faculty/f/k/fkw/rsoc597/UgandaMaps.pdf.
42. Matsumoto PSS, Hiramoto RM, Pereira VBR, Camprigher VM, Taniguchi HH, de Raeffray Barbosa JE, Cortez LRPdB, Fonseca EdS, Guimarães RB, Tolezano JE: **Impact of the dog population and household environment for the maintenance of natural foci of Leishmania infantum transmission to human and animal hosts in endemic areas for visceral leishmaniasis in Sao Paulo state, Brazil**. *PloS one* 2021, **16**(8):e0256534. DOI: https://doi.org/10.1371/journal.pone.0256534.

43. Environmental Systems Research Institute (ESRI): **ArcGIS Desktop Help 10.2 Geostatistical Analyst. https://resources.arcgis.com/en/help/main/10.2/index.html#//009z00000011000000** 2014.
44. Kulldorff M, Heffernan R, Hartman J, Assunçao R, Mostashari F: **A space–time permutation scan statistic for disease outbreak detection**. *Plos med* 2005, **2**(3):e59.
45. Kulldorff M: **Information Management Services, Inc.(2009) SaTScanTM v8. 0: Software for the spatial and space-time scan statistics**. *URL http://www satscan org* 2010.
46. Onozuka D, Hagihara A: **Spatial and temporal dynamics of influenza outbreaks**. *Epidemiology* 2008, **19**(6):824-828.
47. Zhang Z, Chen D, Chen Y, Davies TM, Vaillancourt J-P, Liu W: **Risk signals of an influenza pandemic caused by highly pathogenic avian influenza subtype H5N1: spatio-temporal perspectives**. *The veterinary journal* 2012, **192**(3):417-421.
48. Porta M, ed: **A dictionary of epidemiology**. *Oxford university press* 2014.
49. Elsobky Y, Nganwa D, El Afandi G, Byomi A, Reddy G, Abdalla E: **A quantitative risk assessment to evaluate the efficacy of mitigation strategies to reduce highly pathogenic avian influenza virus, subtype H5N1 (HPAI H5N1) in the Menoufia governorate, Egypt**. *BMC Vet Res* 2021, **17**(1):210. DOI: 10.1186/s12917-021-02917-7.
50. Zhang Z, Chen D, Chen Y, Davies TM, Vaillancourt JP, Liu W: **Risk signals of an influenza pandemic caused by highly pathogenic avian influenza subtype H5N1: spatio-temporal perspectives**. *Veterinary journal (London, England : 1997)* 2012, **192**(3):417-421. DOI: 10.1016/j.tvjl.2011.08.012.
51. El-Shesheny R, Kandeil A, Mostafa A, Ali MA, Webby RJ: **H5 Influenza Viruses in Egypt**. *Cold Spring Harbor Perspectives in Medicine* 2020:a038745.
52. Salaheldin AH, Kasbohm E, El-Naggar H, Ulrich R, Scheibner D, Gischke M, Hassan MK, Arafa A-SA, Hassan WM, El-Hamid A: **Potential biological and climatic factors that influence the incidence and persistence of highly pathogenic H5N1 avian influenza virus in Egypt**. *Frontiers in microbiology* 2018, **9**:528.
53. Arafa A, El-Masry I, Kholosy S, Hassan MK, Dauphin G, Lubroth J, Makonnen YJ: **Phylodynamics of avian influenza clade 2.2. 1 H5N1 viruses in Egypt**. *Virology journal* 2016a, **13**(1):1-11.
54. ELbayoumi KM, Mahgoub K, Mekky HM, Hassan ER, Amin Girh Z, Maatouq AM, El-Samadony HA, Rabie NS, MAA A KM: **Molecular detection of H5N1, H9N2 and Newcastle disease viruses isolated from chicken in mixed infection in Egypt**. *World Applied Sciences Journal* 2013, **27**(1):44-50.
55. Stallknecht DE, Shane SM, Kearney MT, Zwank PJ: **Persistence of avian influenza viruses in water**. *Avian diseases* 1990, **34**(2):406-411.
56. Si Y, de Boer WF, Gong P: **Different environmental drivers of highly pathogenic avian influenza H5N1 outbreaks in poultry and wild birds**. *PLoS One* 2013, **8**(1):e53362. DOI: 10.1371/journal.pone.0053362.
57. Gafi: **"Industrial Zones of Governorate". Ministry of Investment Egypt. Archived from the original on 2018-11-23. Retrieved 23 November 2018.** . 2018. DOI: https://www.gafi.gov.eg/English/StartaBusiness/InvestmentZones/Pages/Industrial-Zones.aspx

58. Norström M, Pfeiffer DU, Jarp J: **A space-time cluster investigation of an outbreak of acute respiratory disease in Norwegian cattle herds**. *Preventive veterinary medicine* 1999, **47**(1-2):107-119. DOI: 10.1016/s0167-5877(00)00159-8.

59. Webster RG, Govorkova EA: **H5N1 influenza—continuing evolution and spread**. *New England Journal of Medicine* 2006, **355**(21):2174-2177.

60. Peyre M, Samaha H, Yilma Jobre Makonnen AS, Abd-Elnabi A, Galal S, Ettel T, Dauphin G, Lubroth J, Roger F, Domenech J: **Avian influenza vaccination in Egypt: limitations of the current strategy**. *Journal of molecular and genetic medicine: an international journal of biomedical research* 2009, **3**(2):198.

61. Vergne T, Grosbois V, Yilma Jobre AS, Abd El Nabi A, Galal S, Kalifa M, Abd El Kader S, Dauphin G, Roger F, Lubroth J: **Avian influenza vaccination of poultry and passive case reporting, Egypt**. *Emerging infectious diseases* 2012, **18**(12):2076.

Tables

Tables 1 to 3 are available in the Supplementary Files section.

Figures

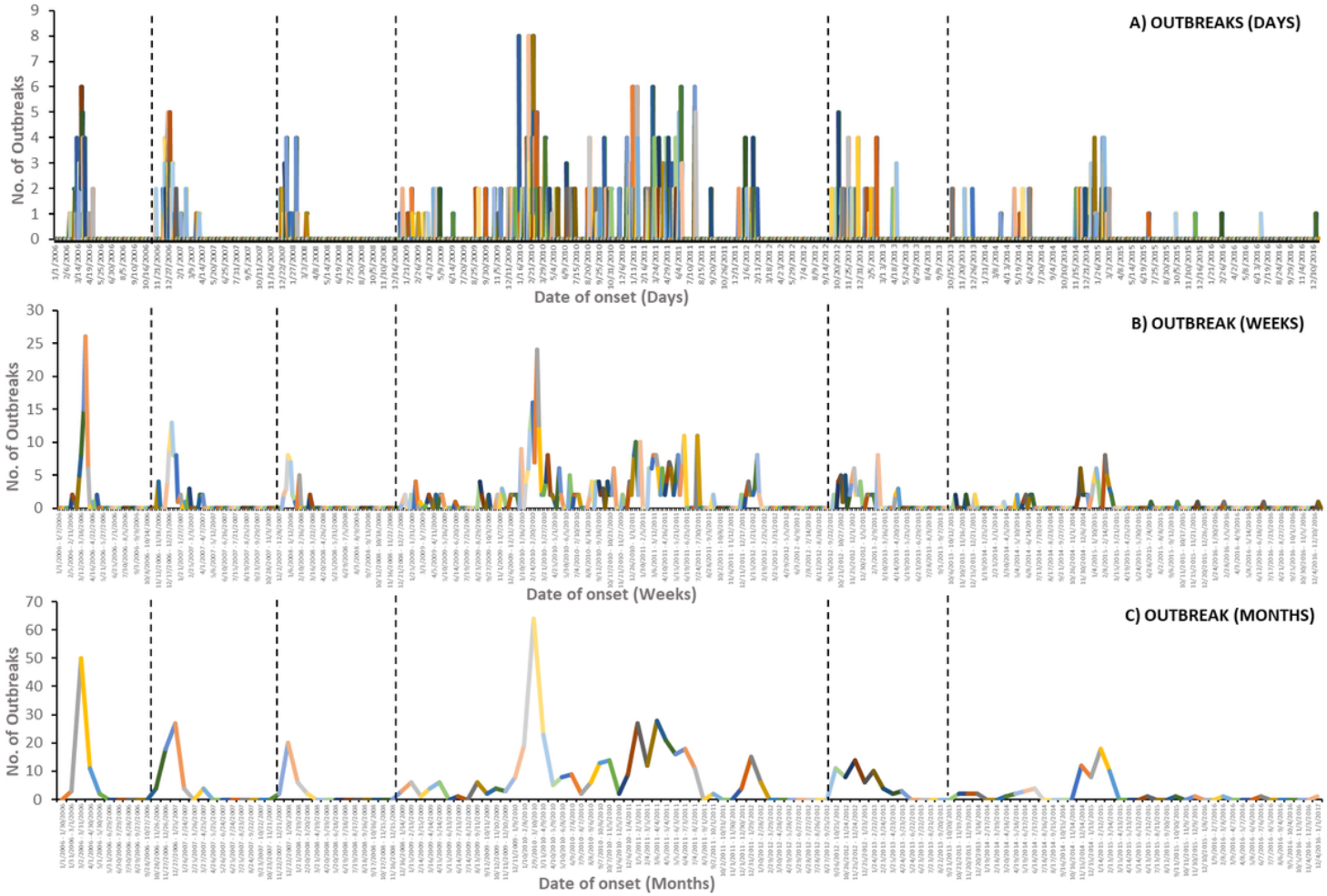

Figure 1

Epidemic curves of outbreaks of highly pathogenic avian influenza subtype H5N1 in Menofia governorate from January 2006 to December 2016, illustrating A) daily, B) weekly, and C) monthly frequency of outbreaks as a function of time. Vertical lines delineate the six epidemic waves

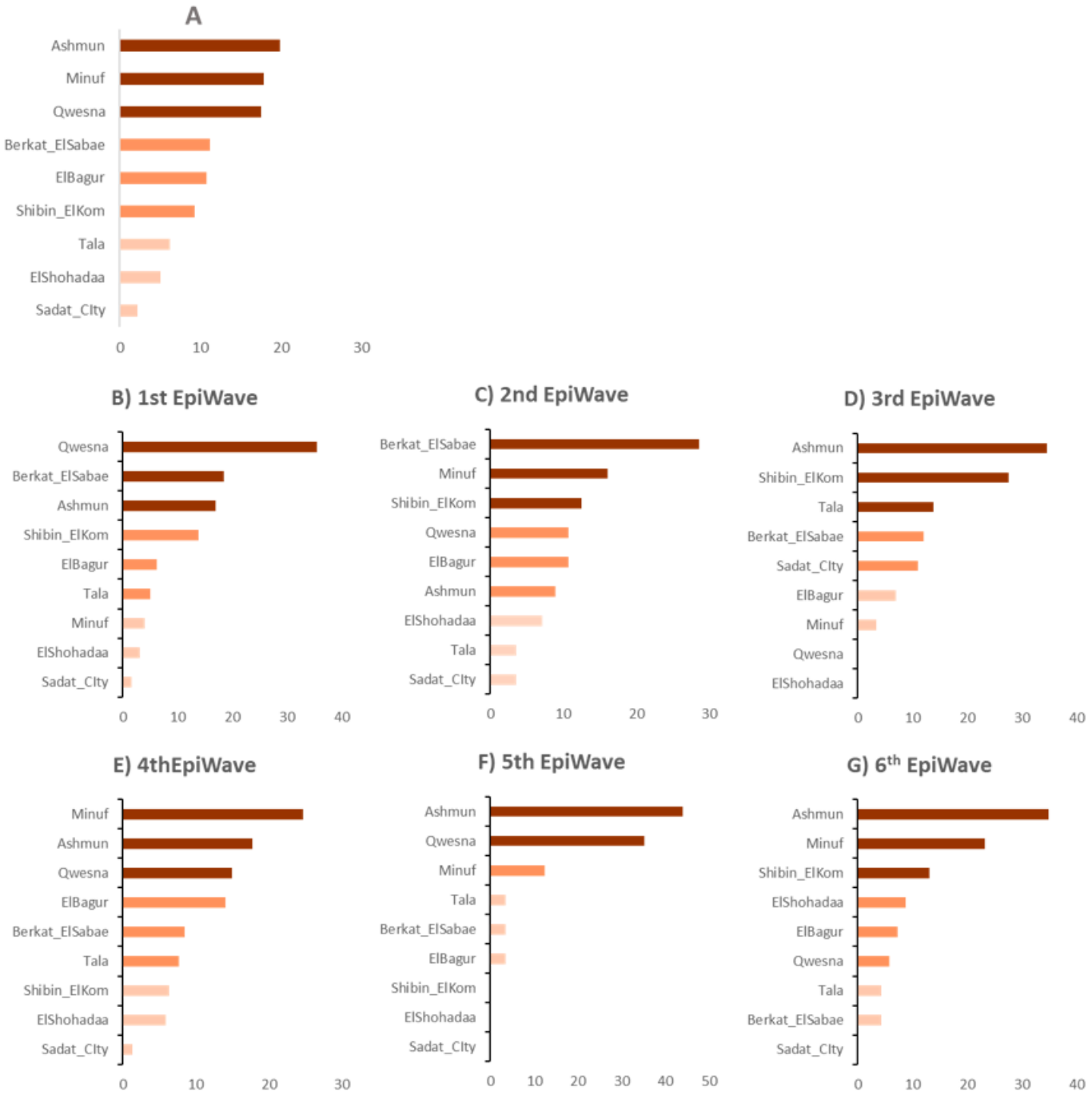

Figure 2

A) Spatial Distribution of HPAI H5N1 outbreaks in Menofia governorate in the period from 2006 to 2016 (B, C, D, E, F, and G are representing the six epidemic waves).

*Vertical axis represents the cities, while horizontal axis represents the total no. of outbreaks.

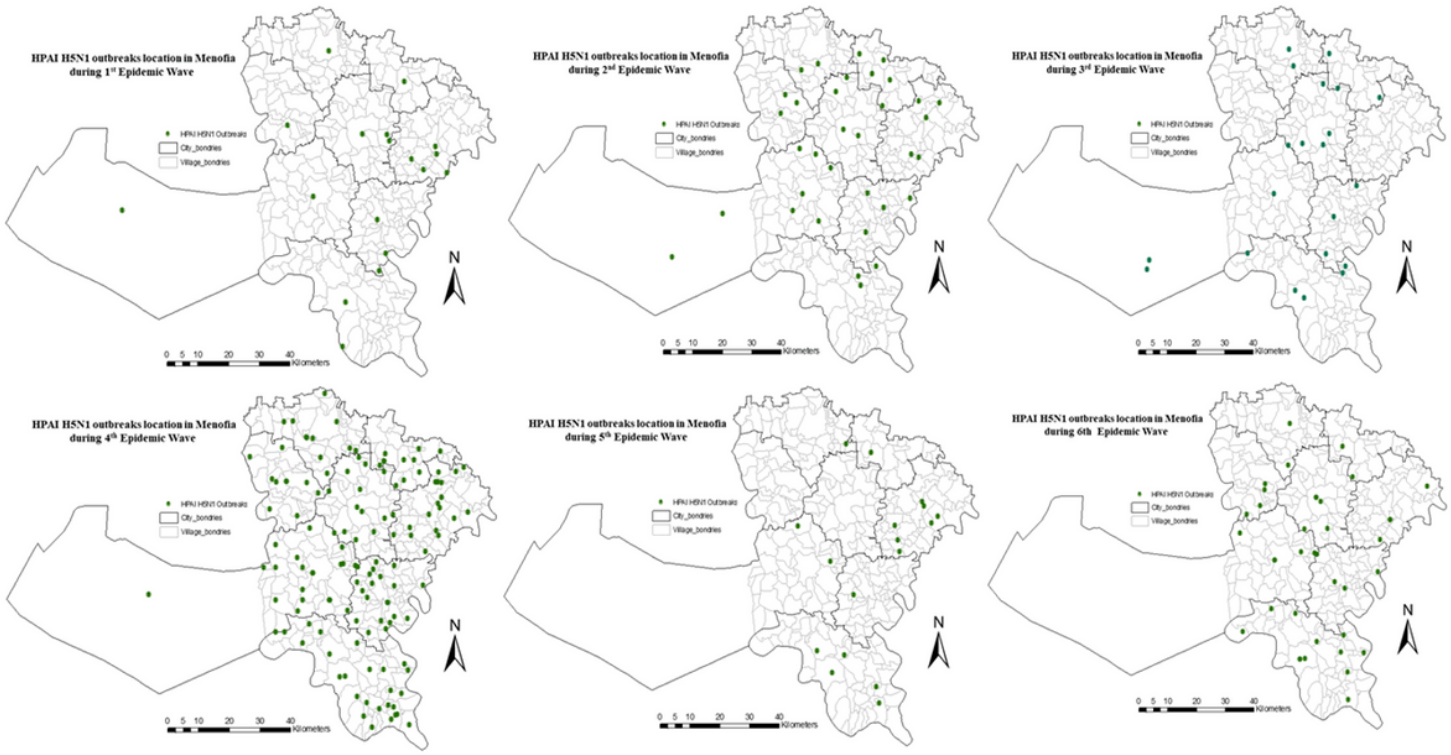

Figure 3

Spatial distribution of HPAI H5N1 outbreaks in Menofia governorate were divided into corresponding subsets according to the epidemic waves and depicted in the village-based map for visual comparison using ARCGIS 10.5 software (ESRI, Redlands, CA, USA).

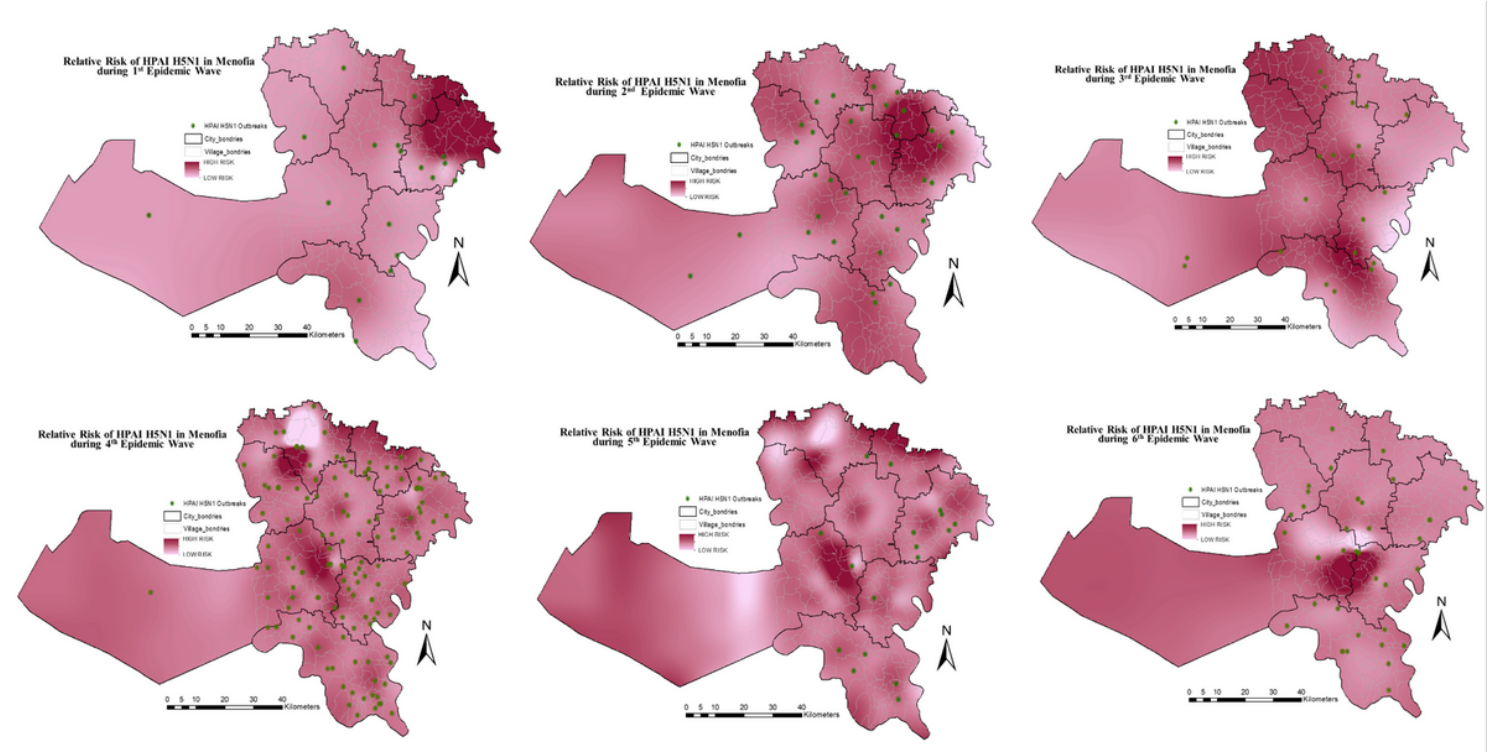

Figure 4

Raster risk map showing interpolated spatial prediction surface of HPAIH5N1 outbreak risk, based on ordinary kriging with ArcMap version 10.1 (ESRI, Redlands, CA, USA). Daily outbreaks of highly pathogenic avian influenza subtype H5N1 over six epidemic waves were represented by light green dots and outbreak Relative risk from spatial analysis highlighted in monochromatic red (the higher the risk, the darker the color).

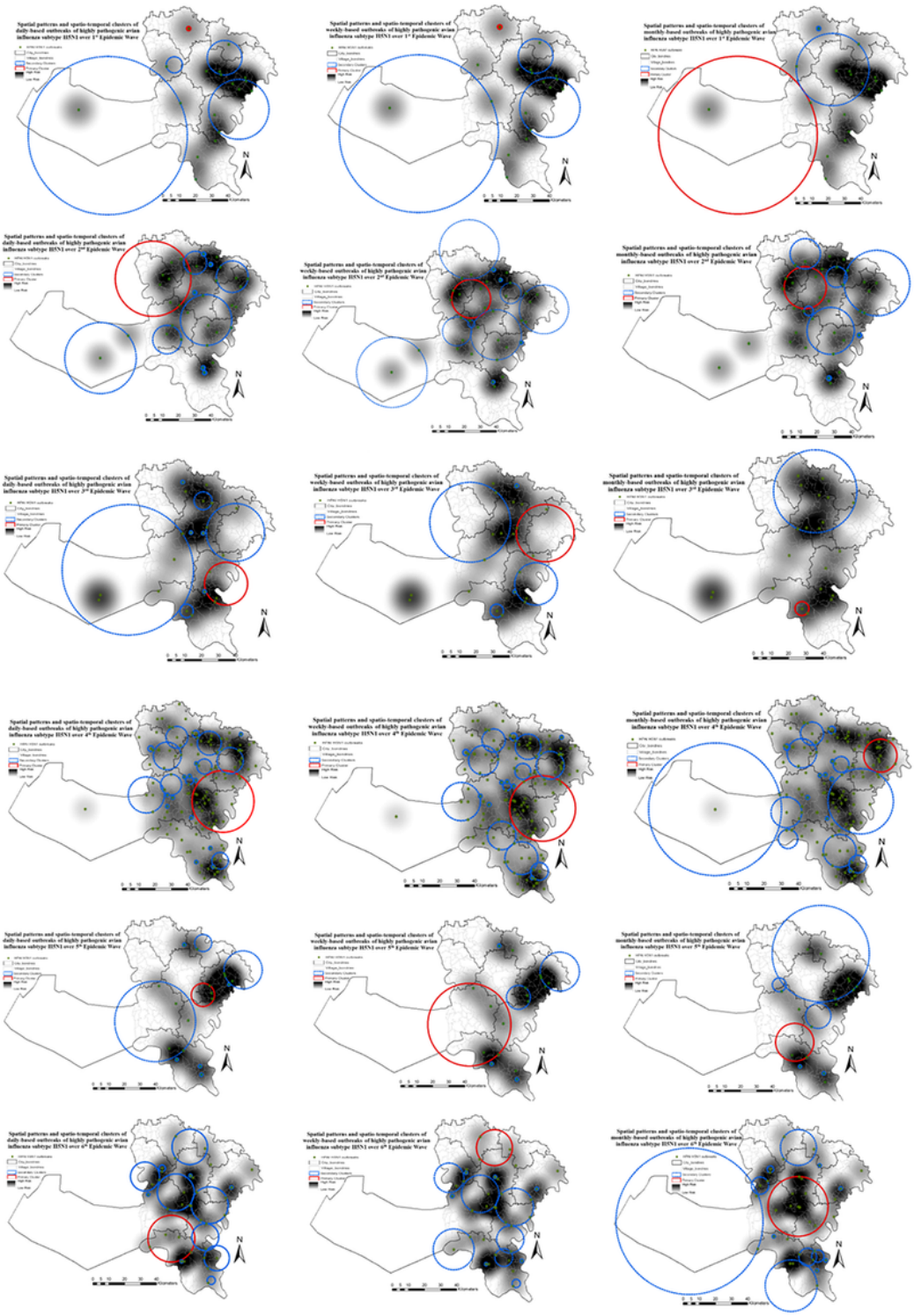

Figure 5

Spatial patterns and spatio-temporal clusters of daily, weekly, and monthly based outbreaks of highly pathogenic avian influenza subtype H5N1 over six epidemic waves in Menofia governorate. Outbreaks represented by light green dots and outbreak density from adaptive kernel density estimation highlighted in monochromatic grey (the higher the density, the darker the color). Significant spatio-temporal clusters

detected from the space–time permutation scan statistics are illustrated by the most likely cluster (red circle) and by a secondary cluster (blue-dashed circles).

Supplementary Files

This is a list of supplementary files associated with this preprint. Click to download.

- 1.Tables.xlsx